COUPLING CONDITIONS FOR LES WITH DOWNSTREAM RANS FOR THE PREDICTION OF INCOMPRESSIBLE TURBULENT FLOWS

Dominic von Terzi
Institut für Hydromechanik, Universität Karlsruhe
Kaiserstraße 12, D-76131 Karlsruhe, Germany
terzi@ifh.uni-karlsruhe.de

Jochen Fröhlich
Lehrstuhl für Strömungsmechanik, Technische Universität Dresden
George-Bähr-Straße 3c, D-01069 Dresden, Germany
jochen.froehlich@tu-dresden.de

ABSTRACT

Interfacing Large Eddy Simulation (LES) with a downstream Reynolds-Averaged Navier–Stokes (RANS) zone for incompressible flows is investigated. The mean velocity fields are matched at the predefined interface and velocity fluctuations of the LES zone are allowed to leave the domain by employing a convective boundary condition. For incompressible flows, in addition, it is also necessary to prescribe conditions for the pressure or an equivalent variable. Two situations are considered: (i) The instantaneous pressure is solved globally within the union of the LES and RANS domains and (ii) the pressure fields are completely decoupled. For the latter, several alternatives of handling the issue of mass conservation at the interface were studied. The performance of the different methods is scrutinized for turbulent channel flow and the flow over periodic hills. It was found that for the first test case the pressure coupling was uncritical whereas, for the hill flow, decoupling of the pressure with explicitly enforced mass conservation at the interface yielded the best and, for some situations, the only acceptable results.

INTRODUCTION

Reynolds-Averaged Navier–Stokes (RANS) calculations are able to deliver reliable results for many flows encountered in applications of engineering interest. In situations where these are not sufficient, Large Eddy Simulation (LES) is the next best choice. For LES, the large-scale motion is computed directly and only the small-scale motion is modeled, hence information on large coherent structures can be gained and less strict modeling assumptions need to hold. The price to pay is a substantially higher computational cost. In fact, it may be so high that LES is not affordable for a very complex high-Reynolds number flow or an extensive parameter study. A remedy is the coupling of LES and RANS calculations. Such a hybrid method restricts the use of the more expensive LES to regions of the flow field where RANS predictions are likely to be inadequate, e.g. in regions where the effects of large coherent structures are of interest.

The interfacing of LES with a downstream RANS zone considered here can be very instructive as an intermediate step towards wall-modeling for LES, but it is also of practical interest in its own right. This is the case for flows where changes in the mean pressure field and/or geometry far downstream of the region of primary interest have a sufficiently strong upstream influence. For such kind of flows, a simple outflow condition cannot be applied close to the region of interest as was shown for a swirl stabilized model combustor by Pierce & Moin (1998). However, lengthening the domain by adding a RANS zone and hence including the downstream effects may be an attractive alternative to more complex boundary conditions (von Terzi *et al.*, 2005).

VELOCITY COUPLING

For LES-to-RANS type boundaries in flows with stationary statistics, the RANS zone can and should only provide mean values, whereas the LES delivers a time-dependent solution. Therefore, the role of the interface is to allow for mean flow information to propagate upstream and for the fluctuations to leave the LES domain without reflections. To this end, a general and parameter-free method can be applied (von Terzi, Fröhlich & Mary, 2006) that couples the explicitly Reynolds-averaged variable at the LES outflow directly to the RANS inflow boundary, whereas fluctuations are convected out of the LES domain using a one-dimensional, linear convection equation:

$$\frac{\partial \phi}{\partial t} + U_n \frac{\partial \phi}{\partial n} = 0 \qquad (1)$$

where n is the direction normal to the interface, $U_n = \langle \overline{u}_n \rangle$ the averaged velocity in the n-direction, and ϕ the resolved fluctuations of the quantity to be coupled. For incompressible flow, only the resolved velocities are coupled this way, hence $\phi = \overline{u}_i' = \overline{u}_i - \langle \overline{u}_i \rangle$. Here, the overbar denotes the filter implied by LES and the brackets represent the Reynolds average which is explicitly applied in any homogeneous spatial direction of the interface plane and in time. The physical meaning of (1) is that the downstream transport of fluctuations across the interface is dominated by convection. For this to be true,

$$U_n > 0 \quad \text{and} \quad U_n \gg \left| \overline{u}_n' \right| \qquad (2)$$

In addition, laminar and modeled turbulent diffusion across the interface must be negligible which, however, is uncritical for turbulent flows and adequately resolved LES.

The coupling condition of (1) is implemented in its discrete form using a first-order upwind difference in the n-direction (index j along a grid line normal to the interface) and a so-called $\theta-$scheme (Tannehill *et al.*, 1997) with

$0 \leq \theta \leq 1$ in time ($t = m\ \Delta t$):

$$\begin{aligned} \phi_j^{m+1} &= C_1\ \phi_j^m + C_2\ \phi_{j-1}^m + C_3\ \phi_{j-1}^{m+1} \qquad (3) \\ C_0 &= 1 + \theta\ \widetilde{U}_n \\ C_1 &= \Big(1 - (1-\theta)\ \widetilde{U}_n\Big) / C_0 \\ C_2 &= \Big((1-\theta)\ \widetilde{U}_n\Big) / C_0 \\ C_3 &= \theta\ \widetilde{U}_n / C_0 \end{aligned}$$

where, for a Finite Volume method, the interface is located at the face between the cells with index j (RANS-side) and $j-1$ (LES-side). For $\theta = 0.5$, as chosen for all simulations presented here, this results in the implicit second-order accurate trapezoid rule. The parameter

$$\widetilde{U}_n = U_n\ \Delta t / \Delta n \qquad (4)$$

is the Courant–Friedrichs–Lewy (CFL) number for the convective problem. The resulting coupling conditions are then

$$U_{j-1}^{m+1} = \langle \overline{u}_{j-1}^{m+1} \rangle \qquad (5)$$

for the streamwise velocity U at the inflow boundary of the RANS calculation and

$$\overline{u}_j^{m+1} = U_j^{m+1} + \overline{u}_j'^{m+1} \qquad (6)$$

for the resolved streamwise velocity $\overline{u}$ at the LES outflow boundary, with $\overline{u}'$ obtained from (3) using a lower bound for $\widetilde{U}_n$ of 10^{-14} to ensure $U_n > 0$. All other velocity components are computed accordingly. Setting $C_1 = C_2 = 0$ and $C_3 = 0.98$ in (3), recovers the *ad hoc* formula for the so-called enrichment strategy of Quéméré & Sagaut (2002). In addition to the downstream RANS considered here, they successfully applied this technique also as a wall-model for LES by placing the RANS zone between the LES zone and the wall.

PRESSURE COUPLING

For incompressible flows with well-posed boundary conditions, mass conservation inside the fluid domain is implicitly enforced through the pressure field or an equivalent constraint variable, e.g. the streamfunction. These variables are governed by a Poisson-type equation such that the convective condition (1) cannot be applied to their fluctuations and a different way of coupling the LES and RANS domains needs to be devised. In the following we restrict ourselves to formulations involving the pressure. Two distinct possibilities of handling this variable at the interface are scrutinized.

One possibility is to solve the instantaneous pressure globally in the union of the LES and the RANS domains. We denote this case C4 in order to keep the notation of von Terzi *et al.* (2006). It is a strong coupling that enforces instant mass conservation in the complete fluid domain. If the algorithm for the Poisson solver employed uses a domain decomposition technique no adjustment to the algorithm is necessary making this a very attractive approach. However, some turbulence models, in particular most of the subgrid-scale models employed for LES, represent only the deviatoric part of the unresolved stresses. As a consequence, a common interpretation of the pressure in the corresponding momentum equations is that of a *modified pressure*, where the missing isotropic term of the unresolved stresses is implicitly added to the physical pressure. If this is the case on any side of the LES–RANS interface, then the sudden change in physical meaning of a pressure solved continuously may cause complications.

An alternative approach is to decouple the pressure fields of the LES and RANS domains completely. In this case, both the velocity and pressure fields are discontinuous at the interface and mass conservation across this boundary is not guaranteed. Ignoring the mass conservation issue is the method identified as case P1 below. P1 constitutes a weak coupling since by matching the averaged velocities at the interface, the mean mass flux is maintained. Instantaneously, however, this is true only if the net mass transport of the fluctuations across the interface sums up to zero at each instant in time. This is likely not to be the case at startup of a simulation, when the explicit time average has not converged yet, and for situations where (2) is violated at the interface, e.g. close to walls and for reverse flow. As a consequence of a lack of instantaneous mass conservation, the boundary conditions for the Poisson solver become ill-posed and the solver converges poorly or not at all.

The problem of an integral mass flux imbalance is not limited to LES/RANS coupling, but occurs routinely with projection methods for incompressible flow. As a remedy, a global mass flux correction is applied computing the mass flux over all inflow boundaries $\dot{m}_{in}$ and calculating the actual mass flux over all exit boundaries $\dot{m}_{out}$ due to the uncorrected exit velocities u_i^*. All velocity components at all outflow cells can then be scaled with the same factor

$$u_i = f_m\ u_i^* \qquad \text{with} \qquad f_m = \frac{|\dot{m}_{in}|}{\dot{m}_{out}} \qquad (7)$$

In practical simulations, the mass flux ratio f_m in (7) is usually very close to one. This "global correction" can also be applied to the velocities constructed with (5) and (6) at the LES/RANS interface. For the LES boundary cells, one needs to replace $\dot{m}_{out}$ in (7) with the mass flux leaving the LES domain $\dot{m}_{LES}$. Conversely, the velocities in the RANS boundary cell are then scaled using the magnitude of the mass flux entering the RANS domain $|\dot{m}_{RANS}|$. The simulation with decoupled pressure and a global mass flux correction is called case P2 below.

For coupling of LES and RANS in case of complex geometries, we might have multiple embedded LES domains making the global correction cumbersome, if not impossible. Hence, a local approximation to the global flux correction above is proposed here with $|\dot{m}_{in}|$ in (7) being replaced, at each simply connected interface, by

$$\dot{m}_{interface} = 1/2\ (\dot{m}_{LES} + |\dot{m}_{RANS}|) \qquad (8)$$

with $\dot{m}_{LES}$ and $\dot{m}_{RANS}$ determined by integration over the corresponding interface. A simulation using this "local correction" is denoted as case P3.

TURBULENCE MODELS AND NUMERICAL METHOD

For all cases presented here, the Smagorinsky model and the Spalart–Allmaras model are used for the LES and RANS regions, respectively. The constant in the Smagorinsky model was chosen as $C_s = 0.065$. For the RANS model, a transport equation for a modified turbulent viscosity $\widetilde{\nu_t}$ is solved. This equation requires a reasonable inlet-type boundary condition at the interface. It is provided by solving the transport equation also in the LES domain, albeit using the explicitly Reynolds-averaged velocities.

The simulations were performed with the Finite Volume flow solver LESOCC2 (Hinterberger, 2004) developed at the

Institute for Hydromechanics at the University of Karlsruhe. It solves the incompressible time-dependent filtered Navier–Stokes equations together with transport equations required for the turbulence models on body-fitted curvilinear block-structured grids. Second-order central differences are used for the discretization of the convection and diffusion fluxes. Only for the convection term in the transport equation for the eddy viscosity the monotonic HLPA scheme is employed. An explicit, low-storage, three-stage Runge–Kutta method is used for time advancement.

TURBULENT CHANNEL FLOW

First, we will compare the different pressure coupling techniques (C4 and P1–3) for fully developed turbulent channel flow at a Reynolds number based on the friction velocity and channel half-width of $Re_\tau = 395$ and based on bulk velocity of $Re = 7000$. For this setup, there exist Direct Numerical Simulation (DNS) data from Moser *et al.* (1999) for comparison and any adverse effect of a coupling can be immediately detected in form of streamwise variations of statistics or reflections of instantaneous quantities (von Terzi *et al.*, 2006).

The domain is divided into three parts: the inflow generator, the principal three-dimensional LES zone and the two-dimensional RANS zone. All quantities are made dimensionless using the channel half-height δ and the bulk velocity U_b at the inlet of the principal LES zone. The inflow generator is a stand-alone LES with periodic boundary conditions in the streamwise direction and a mass flux enforced by volume forces. It provides planes of instantaneous velocities for the inflow of the principal LES zone. For each of the LES zones, the domain size is $2\,\pi \times 2 \times \pi$ in the streamwise (x), wall-normal (y), and spanwise (z) directions, respectively. Grid stretching is employed only in the wall-normal direction. Both domains are discretized using $80 \times 100 \times 80$ cells resulting in a near-wall scaling of $y_1^+ = 1.45$, $\Delta x^+ = 32$, and $\Delta z^+ = 16$. The RANS domain extends over a length of $4\,\pi$ on a stretched grid in the streamwise direction. The same wall-normal grid as for the LES zones is utilized with one cell in the spanwise direction. The time step was $\Delta t = 0.01$ and statistics were sampled over $t = 350\,\delta/U_b$ starting after steady statistics were obtained. All averages were taken in time and the lateral direction.

In figure 1(a) and (b), wall-normal profiles of mean streamwise velocity and resolved longitudinal Reynolds stress in near-wall coordinates are shown. The profiles were taken from the main LES domain in the plane adjacent to the interface. All simulations compare well to the DNS reference data with the coupled simulations exhibiting a slight improvement over the LES data computed on the same grid without coupling.

Figure 1(c) demonstrates the change in meaning of the pressure between DNS, LES, and RANS. Integrating the averaged wall-normal momentum equation results in $\langle p + v'v' \rangle = const.$ as seen for the DNS data. Hence, the mean pressure of the DNS and the mean modified pressure of the LES $\langle p^{LES} \rangle$ change with y. On the other hand, consistent with its modeling assumptions, the Spalart–Allmaras model yields a constant modified pressure in the wall-normal direction, i.e. $p^{RANS} = p + 2K/3 = const.$, where K is the turbulent kinetic energy. However, $2K/3 \neq \langle v'v' \rangle$ due to the near-wall anisotropy. As a consequence, close to the wall, $\langle p^{LES} \rangle$ should differ from p^{RANS} across the interface and some adjustment is to be expected. A simple correction matching p^{RANS} and $\langle p^{LES} \rangle + 2K^{res}/3$ with K^{res} being the resolved turbulent kinetic energy is not adequate, whereas using $\langle p^{LES} \rangle + \langle \overline{v}'\overline{v}' \rangle$ is not general enough to hold for other flow configurations.

Figure 2 provides a closer look at the interface. The streamwise development of instantaneous velocity and pressure and the mean pressure at three different wall-normal locations are shown for cases C4, P1, and P2. The results of P3 are very similar to the other P-cases and are therefore not shown for brevity. The plots demonstrate that the instantaneous velocities fluctuate in the inflow generator, move on through the principle LES domain and leave the latter without reflections. On the RANS side of the interface, a steady mean velocity is obtained. A jump at the interface can be discerned since only the mean values are continuous. The instantaneous pressure behaves alike, albeit with two differences: One is that, in the inflow generator, the mean pressure gradient is missing, since it is represented by the volume forces instead. The other is that for the global pressure coupling (C4) the pressure is continuous at the interface whereas for the P-cases a jump similar to the velocities is clearly visible, but the mean flow gradient is continuous. For case C4, in the near-wall region of the interface, a slight adjustment of the mean pressure can be seen. This is due to the change in modified pressure as discussed above. Since cases P2 and P3 agree well with case P1, mass flux corrections are obviously uncritical for this configuration. In fact, $f_m - 1$ was of the order of 10^{-4}, for both P2 and P3. The global mass flux correction (P2) achieved the best convergence rate of the Poisson solver, whereas the maximum residual of case P3 remained one order of magnitude larger than for all other cases (10^{-5} instead of 10^{-6}).

Contrary to variations in the velocity coupling (von Terzi *et al.*, 2006), the different pressure interfacing methods tested here all delivered excellent results and no clear superiority of any of these methods can be discerned.

FLOW OVER PERIODIC HILLS

The channel flow is a sensitive but uncritical test case since the flow is fully developed so that no downstream information is really needed for the upstream LES. This is different for the flow over periodic hills. This configuration was devised by Mellen *et al.* (2000) and detailed reference data were presented by Fröhlich *et al.* (2005). The Reynolds number based on the hill height h and the bulk velocity over the crest is $Re_b = 10595$. The distance from hill to hill is $9h$, the domain height $3.036h$, and the width $4.5h$. As with the channel flow, the simulation is divided into three distinct zones (figure 3). The first zone is computed with LES using wall functions and periodic boundary conditions in the downstream direction. $200 \times 64 \times 92$ cells are used in the downstream, wall-normal and lateral directions, respectively. This zone provides reference LES and inflow data. For the second zone, LES is performed using the same resolution as in Zone 1. At a pre-defined location, the simulation switches from LES to RANS, and the third zone with a two-dimensional grid begins. At the RANS outflow, Neumann boundary conditions are applied. $\Delta t \approx 3 \times 10^{-3}$ and the total simulation time was roughly $390\,h/U_b$. Two locations for the LES/RANS interface are considered: (i) on the crest of the hill and (ii) before the crest of the hill as illustrated in figure 3.

For the interface placed on the crest, all methods yielded excellent results making this an uncritical test. The interface at $x \approx 7$, on the other hand, constitutes a severe challenge. A conventional convective outflow condition at this position,

i.e. no coupling to a RANS calculation, produced strong reflections and regions of separation before the outflow plane, before eventually the solution diverged. The same happened for cases C4 and P1. This could have been expected, in particular, considering the strong fluctuations of large coherent structures in the center of the channel and the slight separation bubble at the bottom of the upstream hill front. Both are likely to cause violations of the assumptions for the velocity coupling stated in (2). Nonetheless, cases P2 and P3, i.e. the decoupled pressure fields with mass flux correction, yielded reasonable results. This is shown in figure 3 for case P3: The mean streamlines reveal that, for the two-dimensional RANS solution, reattachment occurs far too late, consistent with RANS results in the literature showing that this method is inadequate for predicting the separated flow region. However, the RANS zone successfully provides the upstream LES domain with the pressure and mean velocity information due to the streamline curvature induced by the hill rising behind the interface. Therefore, the LES in Zone 2 is able to deliver results similar to the reference solution of Zone 1, albeit with a slightly longer recirculation region. Both reattachment lengths of $4.1\,h$ and $4.3\,h$ for Zone 1 and 2, respectively, are close to the reference value of 4.6 to $4.7\,h$ of Fröhlich *et al.* (2005). The instantaneous velocity contours show that the RANS flow field is indeed steady, whereas the unsteady velocities on the LES-side of the interface leave the domain without any obvious reflections.

More quantitatively, in figure 4, profiles of mean streamwise velocity and resolved Reynolds stresses obtained from simulations P2 and P3, pure LES on the same grid, and a reference LES of Breuer & Jaffrézic (2005) employing twelve million cells are compared for selected downstream locations. The region of primary interest for the hill flow is arguably the recirculation region as shown in plots (a) and (d)–(f). Differences to the reference LES can be expected for the mean flow and must be expected for the resolved fluctuations due to the coarser resolution, but these are tolerably small. Differences between the coupled simulations P2 and P3 compared to the stand-alone LES cannot be discerned for the mean flow and are small for the resolved stresses where they constitute a slight improvement. Even in close proximity to the interface mean flow deviations remain small (figure 4b). The temporal spectrum of the streamwise velocity at a point in the LES domain right at the interface is shown in figure 4(c). No artificial peaks in the spectrum appear which might be generated by the presence of the interface. They compare well to the reference spectra at nearby locations of Fröhlich *et al.* (2005).

Other than for the channel flow simulations, the flux correction is crucial for the hill flow and was substantially larger ($f_m - 1 = O(10^{-3})$). Overall, the convective velocity coupling with decoupled pressure fields and mass flux correction achieved the main objective of any LES/RANS coupling: the LES region was shortened without deterioration of the results in regions of interest. The rear of the hill was then computed using a two-dimensional RANS calculation, i.e. a fraction of the number of cells in this region of lesser interest was employed.

CONCLUSION

Coupling of LES with a downstream RANS at a sharp interface was investigated for incompressible flows. On the LES-side of the interface a convective condition (von Terzi *et al.*, 2006) was applied to the velocity fluctuations whereas the explicitly averaged velocity was directly coupled to its counterpart in the RANS domain. This method can be regarded as a generalization of the enrichment technique of Quéméré & Sagaut (2002). It is free of parameters and more robust. The method performed well for turbulent channel flow irrespective of the choice of pressure coupling technique.

Depending on the placement of the LES–RANS interface, the hill flow is a challenging test case for coupling LES to a downstream RANS calculation. It was shown that the present velocity coupling can yield very good results. For the pressure, it turned out to be necessary to decouple the two domains completely and then to explicitly enforce mass conservation across the interface. This was achieved by scaling the total velocities on either side. The mass flux to be enforced was either specified globally, e.g. as the mass flux through all inlets of the LES domain, or determined locally by averaging the existing fluxes on both sides of the interface.

The local mass flux correction is more general, easier to implement for complex flow situations, and seems to be very robust. Although this method requires a long startup time until the running averages are sufficiently converged and is less strict in enforcing continuity, decoupling of pressure with a local mass flux correction delivered very promising results for both test cases considered. Taking into account that only the decoupled pressure with mass flux correction delivered acceptable results for all configurations, it is recommended as the standard incompressible complement to the convective velocity coupling.

REFERENCES

Breuer, M. & Jaffrézic, B., 2005, "New reference data for the hill flow test case". http://www.hy.bv.tum.de/DFG-CNRS/.

Fröhlich, J., Mellen, C. P., Rodi, W., Temmerman, L. & Leschziner, M. A., 2005, "Highly resolved large-eddy simulation of separated flow in a channel with streamwise periodic constrictions", *J. Fluid Mech.* **526**, 19–66.

Hinterberger, C., 2004, "Dreidimensionale und tiefengemittelte Large-Eddy-Simulation von Flachwasserströmungen", PhD thesis, University of Karlsruhe.

Mellen, C. P., Fröhlich, J. & Rodi, W., 2000, "Large eddy simulation of the flow over periodic hills", *Proceedings, 16th IMACS World Congress*. Lausanne, Switzerland.

Moser, R. D., Kim, J. & Mansour, N. N., 1999, "Direct numerical simulation of turbulent channel flow up to $\mathrm{Re}_\tau = 590$", *Phys. Fluids* **11**, 943–945.

Pierce, C. D. & Moin, P., 1998, "Large Eddy Simulation of a confined coaxial jet with swirl and heat release", AIAA paper 98-2892.

Quéméré, P. & Sagaut, P., 2002, "Zonal multi-domain RANS/LES simulations of turbulent flows", *Int. J. Num. Meth. Fluids* **40**, 903–925.

Tannehill, J. C., Anderson, D. A. & Pletcher, R. H., ed. 1997, *Computational Fluid Mechanics and Heat Transfer*, 2nd edn., Chap. 4.2.5. Taylor & Francis.

von Terzi, D. A., Fröhlich, J. & Mary, I., 2006, "Zonal coupling of LES with downstream RANS calculations", *Submitted to Theoret. Comput. Fluid Dynamics.*

von Terzi, D. A., Hinterberger, C., García-Villalba, M., Fröhlich, J., Rodi, W. & Mary, I., 2005, "LES with downstream RANS for flow over periodic hills and a model combustor flow", *EUROMECH Colloquium 469, Large–Eddy Simulation of Complex Flows, TU Dresden, Germany, Oct. 6–8, 2005*.

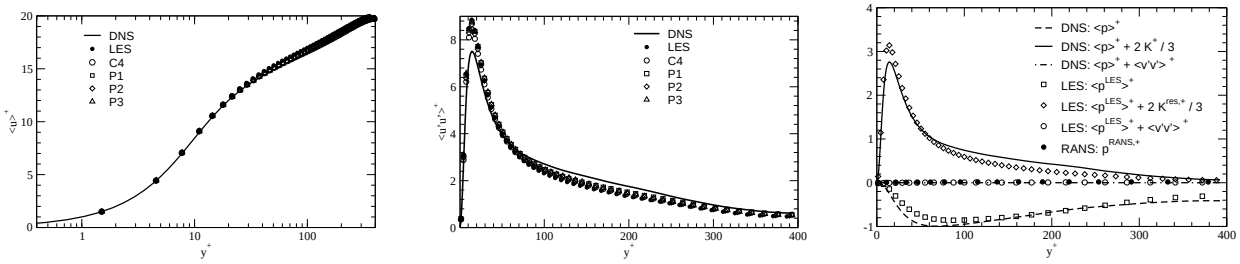

(a) mean streamwise velocity (b) resolved longitudinal Reynolds stress (c) pressure and modified pressure

Figure 1: Turbulent channel flow: Comparison of results with DNS reference data in near-wall scaling and role of modified pressure; profiles for cases C4, P1, P2, and P3 have been obtained at the grid line next to the interface, LES denotes data from the inflow generator.

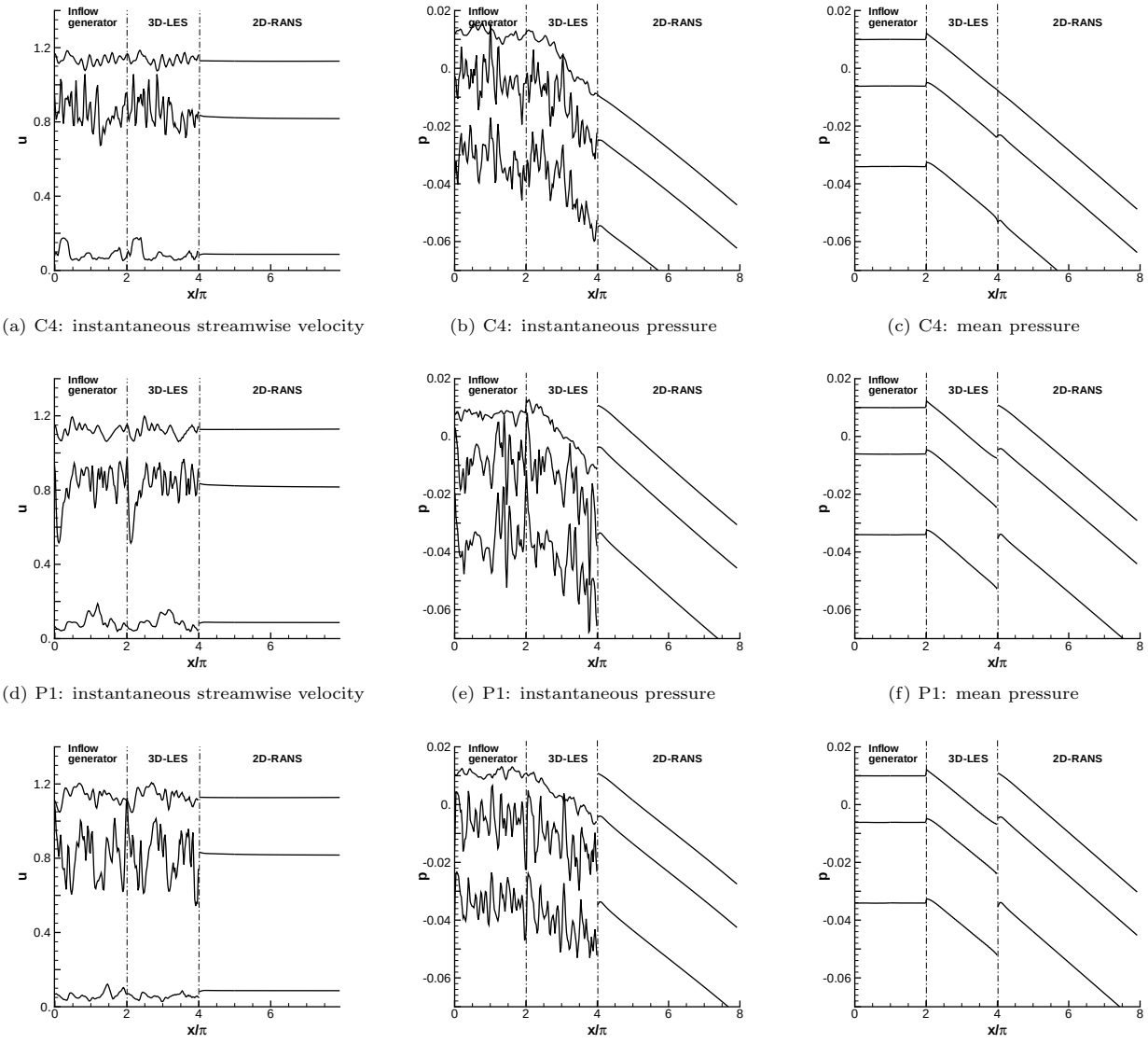

(a) C4: instantaneous streamwise velocity (b) C4: instantaneous pressure (c) C4: mean pressure

(d) P1: instantaneous streamwise velocity (e) P1: instantaneous pressure (f) P1: mean pressure

(g) P2: instantaneous streamwise velocity (h) P2: instantaneous pressure (i) P2: mean pressure

Figure 2: Turbulent channel flow simulations with globally coupled (C4) and decoupled (P1 and P2) pressure fields. Streamwise profiles at different wall-normal locations from top to bottom: center of channel, $y = 0.1$ ($y^+ = 40$), and $y = 0.0037$ ($y^+ = 1.45$); arbitrary offset added to pressure for clarity.

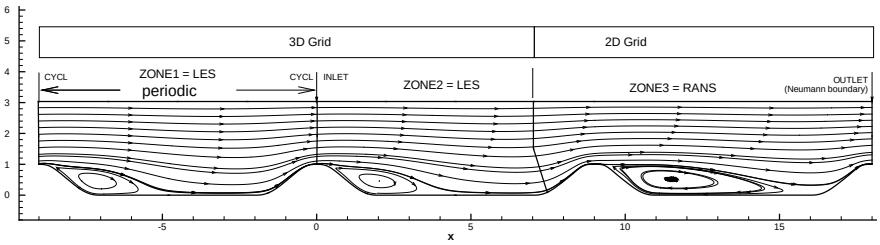

(a) mean streamlines

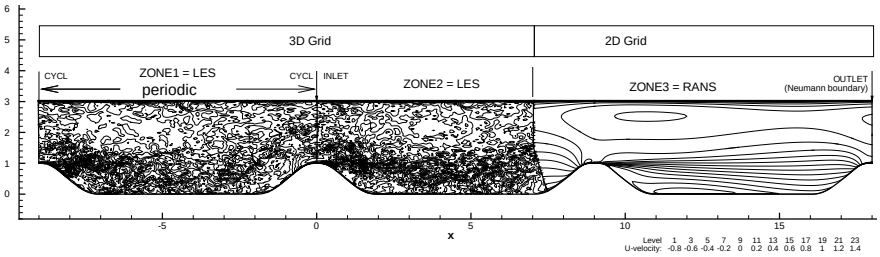

(b) instantaneous streamwise velocity

Figure 3: Flow over periodic hills with interface at $x \approx 7$: Setup of simulation and results for case P3.

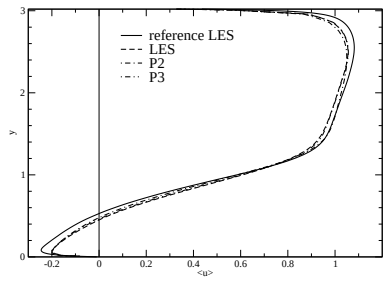

(a) $x = 2$

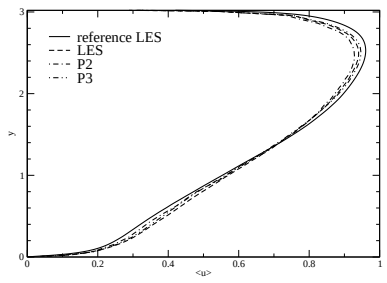

(b) $x = 7$

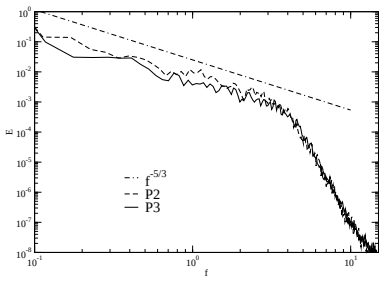

(c) temporal spectrum at $x=7$, $y=2$

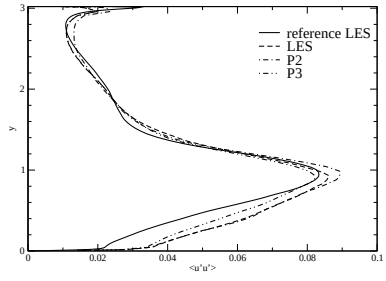

(d) resolved longitudinal Reynolds stress

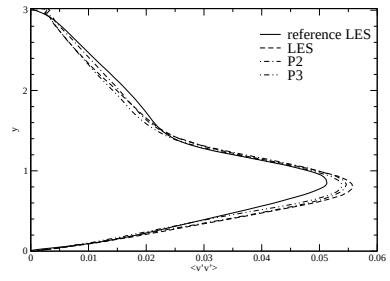

(e) resolved wall-normal Reynolds stress

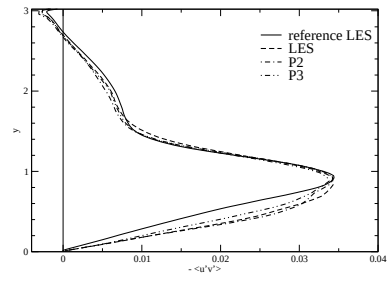

(f) resolved Reynolds shear stress

Figure 4: Flow over periodic hills with interface at $x \approx 7$: Profiles of mean streamwise velocity at selected locations, power spectrum density of streamwise velocity at the interface, and resolved Reynolds stresses at $x = 2$; reference LES from Breuer & Jaffrézic (2005); LES denotes data from the inflow generator.